GLASSES

Ultrahigh-field ^{67}Zn NMR reveals short-range disorder in zeolitic imidazolate framework glasses

Rasmus S. K. Madsen[1]*, Ang Qiao[1]*, Jishnu Sen[2], Ivan Hung[3], Kuizhi Chen[3], Zhehong Gan[3], Sabyasachi Sen[2]†, Yuanzheng Yue[1,4,5]†

The structure of melt-quenched zeolitic imidazole framework (ZIF) glasses can provide insights into their glass-formation mechanism. We directly detected short-range disorder in ZIF glasses using ultrahigh-field zinc-67 solid-state nuclear magnetic resonance spectroscopy. Two distinct Zn sites characteristic of the parent crystals transformed upon melting into a single tetrahedral site with a broad distribution of structural parameters. Moreover, the ligand chemistry in ZIFs appeared to have no controlling effect on the short-range disorder, although the former affected their phase-transition behavior. These findings reveal structure-property relations and could help design metal-organic framework glasses.

Glasses can be obtained through a variety of synthesis and processing routes (*1*, *2*), but rapid cooling of the liquids remains the predominant approach. Melt-quenched (MQ) glasses can be broadly classified as inorganic, organic, and metallic and containing ionic-covalent, covalent, and metallic bonds, respectively. Recently, a fourth family of MQ glasses based on metal-organic frameworks (MOFs) have been reported that have coordination bonds (*3*–*7*). The MQ-MOF glasses are primarily represented by the subset of MOFs called the zeolitic imidazolate frameworks (ZIFs). Their extended tetrahedral network is analogous to silica and zeolites (*8*): Metal ion nodes (such as Zn^{2+} and Co^{2+}) substitute for silicon, and imidazole ($C_3N_2H_3$)–based ligands substitute for oxygen as the bridging unit. A number of ZIF glasses have porosity, which has potential applications in gas capture and storage, and ZIF-62 glass exhibits high transparency and broad mid-infrared luminescence, which have potential photonic applications (*7*, *9*–*13*).

Recent studies have found ZIF-4 ($Zn[Im]_2$) and ZIF-62 ($Zn[Im_{2-x}bIm_x]$)—where Im and bIm are imidazole and benzimidazole, respectively—to be rather stable against crystallization during heat treatment, and that the parent liquids have a higher glass-forming ability compared with most of the network glass-forming liquids (*14*, *15*). The glass-forming ability of ZIF-62 is greater than that of ZIF-4 because its mixed linkers, consisting of imidazole and benzimidazole in some tetrahedra, create greater steric hindrance (*14*). Previous studies explored the structural origin of this high glass-forming ability in both ZIF systems using systematic heat treatments, differential scanning calorimetry (DSC), and x-ray pair distribution function (PDF) analyses (*3*, *14*, *15*). The PDF analyses provided no clear evidence of the appearance of any medium- or long-range order in these glasses after a calorimetric scan, despite the appearance of an exothermic peak immediately before melting (*15*). The enthalpy release was attributed to the densification of the structural network, but the nature and the length scale of the structural changes associated with the decrease of the potential energy remain unclear to date. In addition, although ZIF-4 is chemically simpler than ZIF-62, the former exhibits several features in its temperature-induced phase transitions, including the transition from a low-density amorphous phase (LDA) to a high-density amorphous phase (HDA), as well as the formation and melting of ZIF-zni (which is denser than ZIF-4).

The origin of these multiple transitions remains elusive given the limitations of the analytical techniques available for determining short- and intermediate-range structure in glasses. Raman spectroscopy, $^{13}C/^{1}H$ nuclear magnetic resonance (NMR) spectroscopy, along with x-ray PDFs have been used in the past to study the short-range and medium-range structure of ZIF glasses. Although these studies provided some structural information, no substantial structural difference in the short-range order between the ZIF crystals and corresponding glasses could be identified (*14*). Previous studies showed that the organic ligands in ZIFs remained intact during melt-quenching, implying that the chemical integrity was retained after glass formation (*3*, *5*, *14*). Molecular dynamics simulations indicated that upon melting, the imidazolate-based linkers dissociate and reassociate with Zn atoms through the scission and renewal of Zn–N coordination bonds (*14*, *16*). The $Zn[ligand]_4$ tetrahedral units remain intact in the ZIF glass state after the melt is quenched, and long-range structural disorder is believed to be primarily induced by the distortion of the $Zn[ligand]_4$ intertetrahedral connections (*14*, *16*).

By contrast, the short-range structural order at the scale of the $Zn[ligand]_4$ tetrahedra in MOF glasses remains unknown. Because ^{67}Zn is a quadrupolar nuclide, its NMR spectra can provide not only the information on the chemical shift that is characteristic of the tetrahedral environment of Zn in the ZIFs but also on the electric-field gradient (EFG) at the site of this nuclide in the structure, as encoded in its quadrupolar coupling constant C_Q and asymmetry parameter η_Q. The EFG is a second-rank tensor quantity sensitive to the degree of positional and orientational order at length scales corresponding to the nearest and next-nearest neighbor distances, and possibly to even longer distances (*17*).

Table 1. ^{67}Zn NMR parameters. ^{67}Zn MAS NMR line shape simulation parameters for crystalline and glassy MOFs.

MOF	Lattice site*	δ_{iso} (ppm)	C_Q (±0.2 MHz)	η_Q (±0.05)	Relative fraction (±5%)
ZIF-4 crystal	Zn1	296	5.1	0.6	46
	Zn2	295	3.7	0.6	54
ZIF-62 crystal	Zn1	297	5.8	0.5	48
	Zn2	296	4.0	0.4	52
ZIF-zni crystal	Zn1	288	6.0	0.6	46
	Zn2	290	4.0	0.5	54
ZIF-4 glass	Zn	277	6.9†	N/A	100
ZIF-62 glass	Zn	278	6.5†	N/A	100
ZIF-62b glass	Zn	277	6.8†	N/A	100

*Lattice sites correspond to those designated in structural refinements of ZIF-4, ZIF-62, and ZIF-zni, as reported in (*8*, *28*, *29*). †These values represent the root mean square quadrupolar product $\sqrt{\langle C^2_{Q\eta}\rangle}$.

[1]Department of Chemistry and Bioscience, Aalborg University, 9220 Aalborg, Denmark. [2]Department of Materials Science and Engineering, University of California at Davis, Davis, CA 95616, USA. [3]National High Magnetic Field Laboratory, 1800 E. Paul Dirac Drive Tallahassee, FL 32310, USA. [4]State Key Laboratory of Silicate Materials for Architectures, Wuhan University of Technology, Wuhan 430070, China. [5]School of Materials Science and Engineering, Qilu University of Technology, Jinan 250353, China.
*These authors equally contributed equally to this work.
†Corresponding author. Email: yy@bio.aau.dk (Y.Y.); sbsen@ucdavis.edu (S.S.)

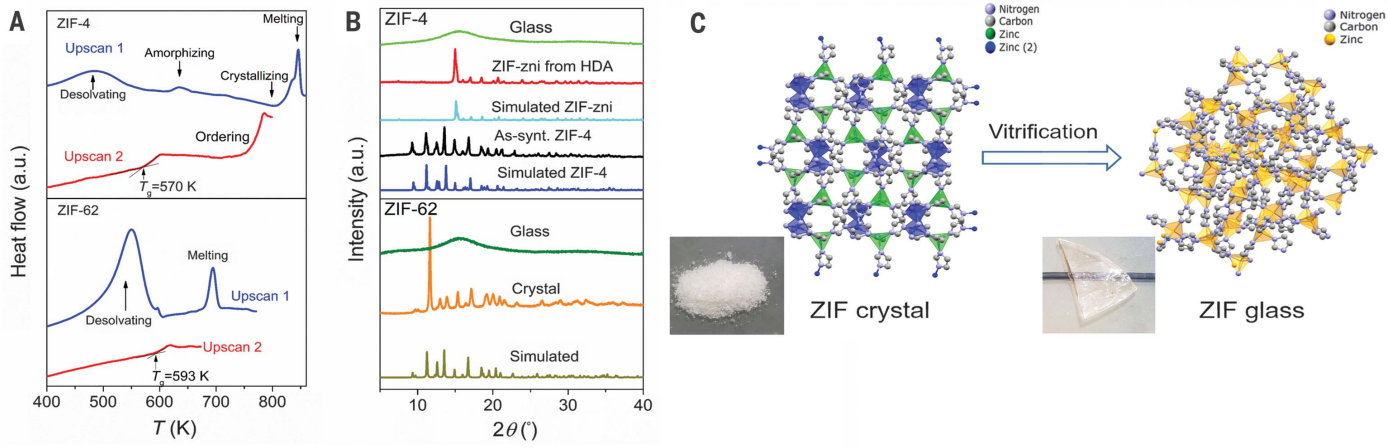

Fig. 1. Phase transitions, glass formation, and glass transition for ZIFs. (**A**) First and second DSC upscans for both (top) ZIF-4 and (bottom) ZIF-62. (**B**) XRD patterns of as-prepared ZIF-4 crystals, ZIF-zni crystals, ZIF-4 glass, ZIF-62 crystals, and ZIF-62 glass. (**C**) Schematic representation of the structural change from crystalline ZIF (powder sample) to its glassy state (transparent bulk sample) during melt-quenching.

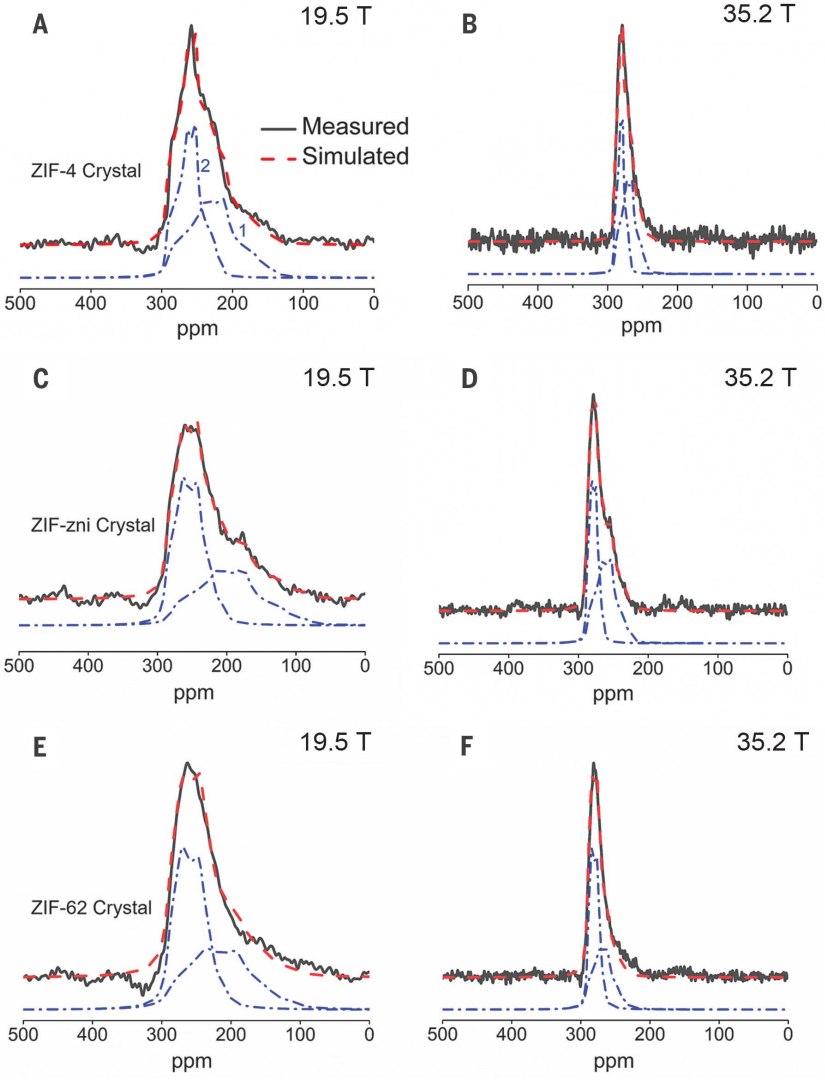

Fig. 2. Short-range order of crystalline ZIFs. (**A** to **F**) Experimental (solid black line) and simulated (dashed red line) ^{67}Zn MAS NMR spectra of [(A) and (B)] crystalline ZIF-4, [(C) and (D)] ZIF-zni, and [(E) and (F)] ZIF-62 collected at 19.5 and 35.2 T. Individual simulation components (dot-dashed blue lines) are vertically offset for clarity.

Only a few ^{67}Zn NMR spectroscopic studies have been reported that analyzed crystalline structures in zinc-based compounds, including Zn-based crystalline MOFs (*18*–*23*), because the ^{67}Zn nuclide has a low gyromagnetic ratio, large quadrupole moment Q, as well as a low natural abundance (*18*). These issues, in combination with the low atomic density of MOFs, necessitated ^{67}Zn NMR spectral data collection at ultrahigh magnetic fields that are ~20 T or higher. We report a comparative structural study of select crystalline ZIFs and their glassy counterparts derived by means of melt-quenching, using ultrahigh-field ^{67}Zn magic-angle-spinning (MAS) NMR spectroscopy at 19.5 and 35.2 T at the National High Magnetic Field Laboratory.

The DSC traces of ZIF-4 and ZIF-62 samples (Fig. 1A) measured the temperature-driven enthalpic responses to the chemical reactions and phase transitions. During the first upscan (from 323 to 863 K), the as-synthesized ZIF-4 crystal underwent solvent release, amorphization, polymorphic transformation to ZIF-zni crystal, and last, melting. Subsequent quenching of the ZIF-zni melt resulted in the formation of a ZIF-4 glass with a glass transition temperature (T_g) of 570 K during the second upscan. By contrast, during upscan 1, the as-synthesized standard ZIF-62 crystal displays the enthalpy responses only to the solvent release and the subsequent melting. After melt-quenching, the second upscan of ZIF-62 glass showed a glass transition with a T_g of 593 K.

To explore the effect of the linker chemistry (the Im/bIm ratio) on the short-range structure, we prepared a ZIF-62 crystal with a higher bIm content (denoted as ZIF-62b) (table S1). Its x-ray diffraction (XRD) patterns confirmed that ZIF-62 and ZIF-62b had the same crystalline structure (fig. S2). The final chemical compositions of ZIF-62 and ZIF-62b were $Zn(Im)_{1.75}(bIm)_{0.25}$ and $Zn(Im)_{1.68}(bIm)_{0.32}$, as determined from ^{1}H liquid NMR measurements (fig. S3). Additionally, we prepared a ZIF-62b glass sample by melt-quenching, which was also subjected to two DSC scans. The increase of bIm in ZIF-62 framework led to an increase of both melting temperature (T_m) and T_g (fig. S4), which is consistent with a previous study (*14*). The XRD patterns of both crystal and glass samples for ZIF-4, -zni, and -62 (Fig. 1B) show the presence of long-range order in crystalline ZIFs and its absence in their glassy counterparts. The vitrification of these ZIF crystals is schematically demonstrated in Fig. 1C.

The ^{67}Zn MAS NMR spectra of the three crystalline ZIFs (ZIF-4, ZIF-62, and ZIF-zni) were obtained at two different magnetic fields, 19.5 and 35.2 T (Fig. 2). Each of these crystals contained two crystallographically distinct Zn sites at a 1:1 ratio, one of which is a more distorted Zn[ligand]$_4$ tetrahedron (*18*). The ^{67}Zn MAS NMR line shapes also necessitated simulation with at least two sites with subequal (within ±5%) relative fractions (Fig. 2); we used the software Dmfit (*24*). For each composition, the spectra collected at both magnetic fields were fitted simultaneously with the same set of NMR parameters: isotropic chemical shift δ_{iso}, the quadrupolar coupling constant C_Q, and asymmetry parameter η_Q. These parameters are listed in Table 1, and the C_Q values for ZIF-4 are in good agreement with those reported in a recent study (*18*).

The data in Table 1 indicated that the δ_{iso} for all Zn sites in all materials varied over a rather narrow range, from ~277 to 297 parts per million (ppm). However, for each crystalline ZIF, the less distorted Zn sites (Zn2) had a smaller C_Q of ~4.0 MHz compared with the more distorted ones (Zn1) characterized by a larger C_Q of ~5 to 6 MHz. These assignments followed the density functional theory–based calculations by Sutrisno *et al.* (*18*). Intriguingly, in spite of having the same composition, the ^{67}Zn C_Q values of the two Zn sites in ZIF-4 crystal are substantially different from those in ZIF-zni crystal. This result may be indicative of the corresponding difference in the topology between these two crystals; ZIF-4 has a *cag* topology and the ZIF-zni has a *zni* topology (*5*). The higher C_Q values of the Zn sites in the ZIF-zni crystal compared with those for the ZIF-4 crystal are also consistent with ZIF-zni possessing a greater variance in the bond angles and lengths for the Zn sites compared with ZIF-4 (tables S2 and S3).

The ^{67}Zn MAS-NMR spectra of the ZIF-4 and ZIF-62 glasses were obtained at both

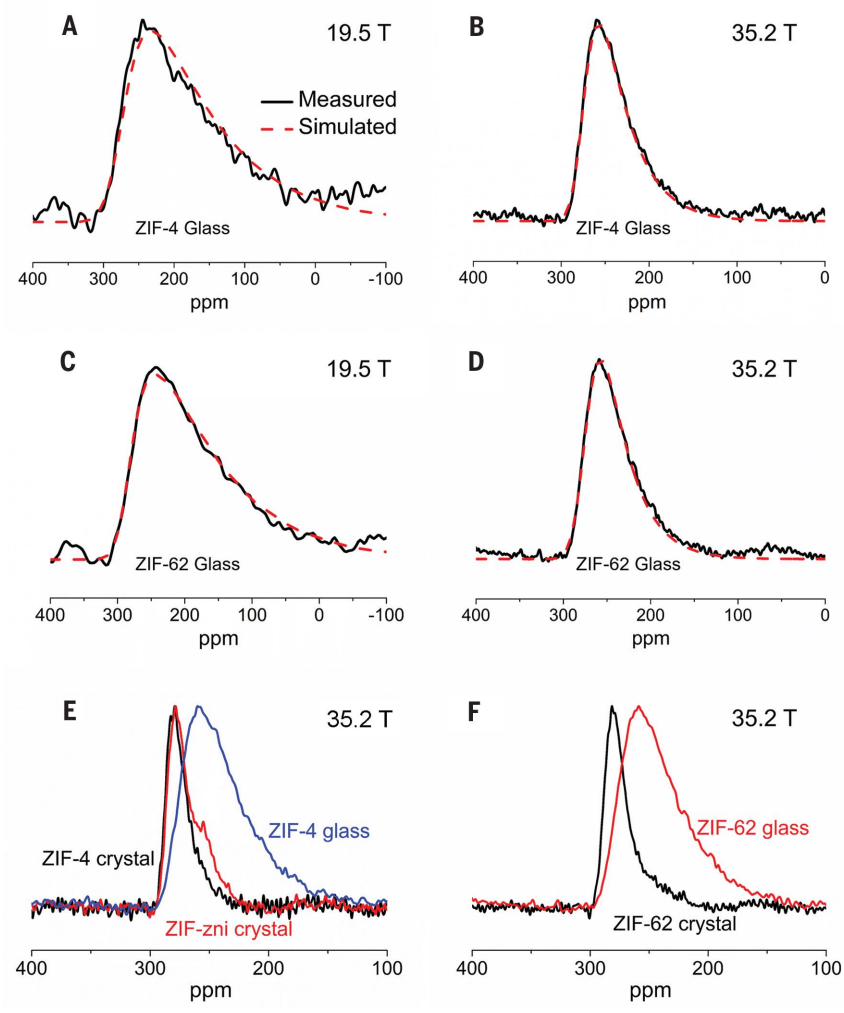

Fig. 3. Comparison of short-range structure between ZIF glasses and crystals. (**A** to **D**) Experimental (solid black line) and simulated (dashed red line) ^{67}Zn MAS NMR spectra for [(A) and (B)] ZIF-4 glass and [(C) and (D)] the standard ZIF-62 glass at different magnetic fields. (**E**) Direct comparison of ^{67}Zn MAS NMR spectra collected at 35.2 T between ZIF-4 crystal, ZIF-zni crystal, and ZIF-4 glass. (**F**) Direct comparison of spectra collected at 35.2 T of ZIF-62 crystal and glass.

19.5 and 35.2 T (Fig. 3, A to D). These spectra had asymmetric line shapes with low-frequency tails that we attributed to a continuous distribution of C_Q characteristic of structural disorder in the glassy state. These ^{67}Zn MAS NMR line shapes were well simulated with δ_{iso} (277 to 278 ppm) similar to that observed in corresponding crystals (288 to 297 ppm) (Table 1) and with a Czjzek distribution of the C_Q parameter (*25*), which yields a root-mean-square quadrupolar product $\sqrt{\langle C^2_{Q\eta}\rangle}$ of ~6.9 MHz for the ZIF-4 glass and ~6.5 to 6.8 MHz for the two ZIF-62 glasses. When taken together, the results in Table 1 indicate that as the ZIF crystals were melt-quenched into glass, the C_Q values increased and displayed a broader distribution, indicating that the structural disorder of the Zn[ligand]$_4$ tetrahedral environment in the glassy state was higher than that in the parent crystals. The ^{67}Zn NMR parameters for all three ZIF glasses were similar (Table 1), implying a similar degree of short-range disorder, despite their differences in the Im/bIm ratio in the ligands.

The disappearance of the two distinct Zn sites characteristic of the ZIF crystals upon melting and vitrification indicates that the scission and renewal of the Zn–N bonds upon melting resulted in structural reconstruction (Fig. 1C and fig. S1). With their three-dimensional network of corner-sharing Zn[ligand]$_4$ tetrahedral units, ZIF glasses are structurally analogous to vitreous silica, but the coordination bonds in ZIF glasses were considerably weaker than the covalent-ionic bonds in silica. (*26*, *27*). The silica glass network would be more rigid than ZIF glasses, and the local structure of the former would be more ordered than that of ZIF glasses. The bulky nature of the organic linkers in ZIF glasses could also cause steric hindrance, thus limiting the ability of the linker to return to its equilibrium position—to the ordered structural state with lower potential energy—upon melt-quenching. The comparison in NMR spectra among ZIF-4 and -zni crystals and ZIF-4 glass (Fig. 3E), and between ZIF-62 crystal and glass (Fig. 3F), shows broadening of the glasses compared with the crystals, and the resonance peaks moved to somewhat lower isotropic chemical shift from crystal to glass. Although the increased broadening corresponds to a high degree of structural disorder in glasses at the short-range scale, the lowering of the isotropic chemical shift is suggestive of a more specific change in the local coordination environment of Zn atoms upon vitrification. Previous Zn K-edge x-ray absorption fine structure and PDF measurements (*5*) indicated that Zn is in tetrahedral coordination with N in both glassy and crystalline ZIFs, and that the Zn–N distance did not change considerably upon vitrification. However, ^{67}Zn solid-state NMR results of Sutrisno *et al.* (*18*) showed that the ^{67}Zn NMR isotropic chemical shift of ZIF-14 (260 ppm) with longer Zn–N distances (2.00 to 2.02 Å) was significantly lower than that of ZIF-8 or ZIF-4 (300 to 315 ppm) characterized by shorter Zn–N distances (1.98 to 1.99 Å). Although further systematic studies are needed to establish this trend, the lower ^{67}Zn NMR isotropic chemical shift of ZIF glasses compared with their crystalline counterparts as observed in the present study could be an indication of an increase in the average Zn–N distance in the former, which is consistent with the corresponding increase in the molar volume upon vitrification.

REFERENCES AND NOTES

1. C. A. Angell, *Science* **267**, 1924–1935 (1995).
2. G. N. Greaves, S. Sen, *Adv. Phys.* **56**, 1–166 (2007).
3. T. D. Bennett *et al.*, *Nat. Commun.* **6**, 8079 (2015).
4. D. Umeyama *et al.*, *Chem. Commun.* **51**, 12728–12731 (2015).
5. T. D. Bennett *et al.*, *J. Am. Chem. Soc.* **138**, 3484–3492 (2016).
6. D. Umeyama, S. Horike, M. Inukai, T. Itakura, S. Kitagawa, *J. Am. Chem. Soc.* **137**, 864–870 (2015).
7. Y. Zhao, S. Y. Lee, N. Becknell, O. M. Yaghi, C. A. Angell, *J. Am. Chem. Soc.* **138**, 10818–10821 (2016).
8. K. S. Park *et al.*, *Proc. Natl. Acad. Sci. U.S.A.* **103**, 10186–10191 (2006).
9. C. Zhou *et al.*, *Nat. Commun.* **9**, 5042 (2018).
10. L. Frentzel-Beyme *et al.*, *J. Mater. Chem. A Mater. Energy Sustain.* **7**, 985–990 (2019).
11. L. Frentzel-Beyme, M. Kloß, P. Kolodzeiski, R. Pallach, S. Henke, *J. Am. Chem. Soc.* **141**, 12362–12371 (2019).
12. M. A. Ali *et al.*, *ACS Omega* **4**, 12081–12087 (2019).
13. A. Qiao *et al.*, *Opt. Lett.* **44**, 1623–1625 (2019).
14. A. Qiao *et al.*, *Sci. Adv.* **4**, eaao6827 (2018).
15. J. Zhang *et al.*, *Chem. Commun.* **55**, 2521–2524 (2019).
16. R. Gaillac *et al.*, *Nat. Mater.* **16**, 1149–1154 (2017).
17. A. P. M. Kentgens, *Geoderma* **80**, 271–306 (1997).
18. A. Sutrisno *et al.*, *Chemistry* **18**, 12251–12259 (2012).
19. K. H. Mroué, W. P. Power, *J. Phys. Chem. A* **114**, 324–335 (2010).
20. T. Bastow, *J. Phys. Condens. Matter* **8**, 11309–11315 (1996).
21. G. Wu, S. Kroeker, R. E. Wasylishen, *Inorg. Chem.* **34**, 1595–1598 (1995).
22. F. H. Larsen, A. S. Lipton, H. J. Jakobsen, N. C. Nielsen, P. D. Ellis, *J. Am. Chem. Soc.* **121**, 3783–3784 (1999).
23. A. S. Lipton, R. W. Heck, P. D. Ellis, *J. Am. Chem. Soc.* **126**, 4735–4739 (2004).
24. D. Massiot *et al.*, *Magn. Reson. Chem.* **40**, 70–76 (2002).
25. J.-B. d'Espinose de Lacaillerie, C. Fretigny, D. Massiot, *J. Magn. Reson.* **192**, 244–251 (2008).
26. R. Gaillac, P. Pullumbi, F.-X. Coudert, *J. Phys. Chem. C* **122**, 6730–6736 (2018).
27. D. C. Clupper, L. L. Hench, *J. Non-Cryst. Solids* **318**, 43–48 (2003).
28. P. Z. Moghadam *et al.*, *Chem. Mater.* **29**, 2618–2625 (2017).
29. R. Banerjee *et al.*, *Science* **319**, 939–943 (2008).

ACKNOWLEDGMENTS

Funding: The authors thank the VILLUM FONDEN (13253) and the NSFC (51802263), China, for financial support. S.S. acknowledges support from the National Science Foundation grant NSF-DMR 1855176. The National High Magnetic Field Laboratory (NHMFL) is supported by the National Science Foundation through NSF/DMR-1644779 and the state of Florida. Development of the 36-T series connected hybrid magnet and NMR instrumentation was supported by NSF (DMR-1039938 and DMR-0603042) and NIH (BTRR 1P41 GM122698). **Author contributions:** Y.Y. and S.S. conceived the project; Y.Y., S.S., R.S.K.M., and A.Q. made the outline of the project. I.H., K.C., and Z.G. performed NMR measurements at NHMFL. J.S. performed all NMR spectral data processing and simulation. A.Q., R.S.K.M., and Y.Y. synthesized the samples and conducted DSC and XRD measurements. Y.Y., S.S., R.S.M., and A.Q. wrote the manuscript, with inputs from I.H., K.C., Z.G., and J.S. **Competing interests:** The authors declare that they have no competing interests. **Data and materials availability:** All data needed to evaluate the conclusions in the paper are present in the paper and/or the supplementary materials. Additional data related to this paper may be requested from the authors.

SUPPLEMENTARY MATERIALS

science.sciencemag.org/content/367/6485/1473/suppl/DC1
Materials and Methods
Figs. S1 to S5
Table S1 to S3
References (*30*–*34*)

6 August 2019; resubmitted 22 January 2020
Accepted 5 March 2020
10.1126/science.aaz0251

Science

Ultrahigh-field ^{67}Zn NMR reveals short-range disorder in zeolitic imidazolate framework glasses

Rasmus S. K. Madsen, Ang Qiao, Jishnu Sen, Ivan Hung, Kuizhi Chen, Zhehong Gan, Sabyasachi Sen and Yuanzheng Yue

Science **367** (6485), 1473-1476.
DOI: 10.1126/science.aaz0251

Glassy metal-organic frameworks

The node-and-linker structure of metal-organic frameworks could enable detailed structural studies of molecular glasses quenched from melts. Zinc-based zeolitic imidazole frameworks exhibit a high propensity for glass formation at conventional cooling rates. Madsen *et al.* used ultrahigh magnetic fields (19.5 and 35.2 tesla) to perform zinc-67 nuclear magnetic resonance of solid samples with magic-angle spinning on three samples with different ratios of imidazole and benzimidazole linkers. The structural disorder of the tetrahedral ligand environment around zinc nodes was higher in the glassy states than in the parent crystals.

Science, this issue p. 1473